Theoretical Study of the Double Proton Transfer in the CHX−XH···CHX−XH (X = O, S) Complexes

Pablo Jaque and Alejandro Toro-Labbé*,†

Departamento de Química Física, Facultad de Química, Pontificia Universidad Católica de Chile, Casilla 306, Correo 22, Santiago, Chile

A theoretical study of double-proton-transfer processes in bimolecular complexes formed by combinations of molecules of the type CHX−XH (X = O, S) is reported. The reactions are rationalized in terms of the energy, chemical potential, and hardness of hydrogen-bonded and isolated species. Sanderson's rule to determine molecular chemical potential and hardness from the values of the constituent fragments is used to characterize the relaxation effects due to hydrogen bonding. In ten formation and seven double-proton transfer processes studied here, the principles of maximum hardness and minimum polarizability are verified. The mechanism for double proton transfer has been analyzed through the force acting on the system to bring reactants into products and the corresponding energy barriers have been qualitatively classified according to its *through bond* or *through space* nature.

1. Introduction

Proton transfer (PT) is one of the simplest and fundamental reactions in chemistry; because it is important in oxidation−reduction reactions in many chemical and biological process, it has been studied extensively.[1−3] There is a growing interest in the study of intrisic properties of both, the H-bonded complexes and the dynamic of the transfer itself, the literature accumulated over the years includes studies based on different ab initio methodologies such as Hartree−Fock (HF) and density functional calculations.[4−11] Most PT studies concerns transfer of a single proton during the reaction, processes in which more than one proton is transferred have been less studied. In this paper we are concerned with the formation of ten cyclic bimolecular complexes formed by combinations of CHX−XH (X = O, S) species and the subsequent double proton transfer (2PT) reactions.

The double proton transfer in formic acid dimer [(HCOOH)$_2$] has been extensively studied from both experimental and theoretical viewpoints;[11−25] it is well-known that it forms strong enough hydrogen bonds so that it is fairly easy to measure their infrared and Raman frequencies.[13−15,17,18] (HCOOH)$_2$ has been used as a model to study key properties of many chemically and biologically important multiproton-transfer systems. On the basic units CHX−XH (X = O, S) that form the complexes in which we are interested here, there are many theoretical and spectroscopic studies of their molecular structure, electronic properties, barriers to internal rotation around the C−X bond, etc.[26−28] The geometrical change of the monomeric units on complexation and the associated energetic stabilization due to formation of hydrogen bonds have also received attention.[16,22,23] Recently, many theoretical studies at various levels of theory have been carried out to predict the structures of the formic acid dimer and the potential energy surface (PES) for the 2PT process. The minimun energy path (MEP) on PES involves a complex set of nuclear displacements: the transfer is initiated by the displacement of heavy atoms bringing the monomer units closer to each other, near the barrier for transfer; at the vicinity of the transition state (TS), the MEP becomes mostly due to hydrogenic motion as the protons are transferred.[19−23] Another interesting feature encountered in PT processes is that electronic charge flows in a direction which is opposite to that of the proton motion, so monitoring the redistribution of electron charges during the dynamical process may give insight about the reaction mechanisms.

In this context, a chemical reaction can be seen as resulting from redistribution of electron density among the atoms in a molecule. Density functional theory (DFT)[29−34] is quite well suited to describe such electronic reorganization processes; it has provided definitions for the chemical potential (μ), molecular hardness (η) and softness ($S = 1/\eta$). The chemical potential characterizes the escaping tendency of electrons from the equilibrium systems while η and S can be seen as a resistance and capacity to charge transfer, respectively. The study of the profiles of μ and η along a reaction coordinate has been shown to be useful in rationalizing different aspects of the progress of chemical reactions, in particular those related to the characterization of transition states.[35−39]

On the other hand, a major focus of attention in the application of DFT to chemical reactivity is the principle of maximun hardness (PMH) that asserts that molecular systems at equilibrium tend to states of highest hardness;[32,40−42] therefore, the PMH can also be helpful in identifying transition states where minimun values of η are expected.[37] Rationalizing the transition states through the PMH leads to establish a bridge connecting electronic and energetic properties, i.e., reaction mechanisms and thermodynamics.[39] This is of considerable theoretical interest since it complements the well-known relationships between kinetic and thermodynamics.[43] Along with this, Chattaraj et al. have proposed a minimun polarizability principle (MPP) which states that the natural direction of evolution of any system is toward a state of minimum polarizability.[44,45] In general the conditions of maximun hardness and minimun polarizability complement the minimun energy

† E-mail: atola@puc.cl.

criterion for molecular stability, and they are criteria that we will use to characterize our systems.

In this paper we investigate the formation of 10 bimolecular complexes from the combination of basic units of the type CHX−XH (X = O, S). Then we focus our attention to the study of synchronous 2PT processes occurring in cyclic complexes. Formation and proton-transfer processes are discussed and analyzed in terms of the change in energy, chemical potential, hardness, and polarizability (α). Characterization of various properties of the transition states of 2PT reactions allows one to identify the specific interactions stabilizing the complexes and helps determine the physical nature of the energy barrier for the simultaneous transfer of two protons.

2. Theory

General Definitions. Within the framework of DFT, the chemical potential and hardness for an *N*-particle system with total energy *E* and external potential $v(\vec{r})$ are defined as follows:[30,33]

$$\mu = \left(\frac{\partial E}{\partial N}\right)_{v(r)} = -\chi \tag{1}$$

and

$$\eta = \frac{1}{2}\left(\frac{\partial^2 E}{\partial N^2}\right)_{v(r)} = \frac{1}{2}\left(\frac{\partial \mu}{\partial N}\right)_{v(r)} \tag{2}$$

As pointed out in eq 1, μ is the negative of the electronegativity χ and it is the Lagrange multiplier associated with the normalization constraint of DFT.[33] In most numerical applications, μ and η are calculated from the knowledge of ionization potential (*I*) and electron affinities (*A*), the following approximate versions of eqs 1 and 2 based upon a three-points finite difference approximation and the Koopmans theorem are widely used:[33]

$$\mu \approx -\frac{1}{2}(I + A) = \frac{1}{2}(\epsilon_L + \epsilon_H) \tag{3}$$

and

$$\eta \approx \frac{1}{2}(I - A) = \frac{1}{2}(\epsilon_L - \epsilon_H) \tag{4}$$

where ϵ_H and ϵ_L are the energies of the highest occupied molecular orbital (HOMO) and the lowest unoccupied molecular orbital (LUMO), respectively. In this paper μ and η are calculated using the expressions involving the molecular orbital energies.

Formation of the Hydrogen Bonded Complex. The formation energy of the hydrogen bonded (hb) species is given by

$$\Delta E_{hb} = E_{hb} - \sum_m^2 E_m \tag{5}$$

where E_{hb} is the energy of the fully optimized hydrogen bonded complex and E_m is the energy of the corresponding fully optimized monomeric species. Although the basis set superposition error (BSSE) may be important in the calculation of the formation energies,[46] it is beyond the scope of this paper. Our main goal here is to discuss the validity of Sanderson's addition scheme[47] in the determination of molecular electronic properties from the corresponding values associated with their nonbonded

TABLE 1: Energy, Chemical Potential, Hardness and Polarizability Values for the Fully Optimized Structures of Monomeric Units[a]

molecule	E	μ	η	α
HC(=O)−OH	−188.820525	−0.1554	0.3138	15.1733
HC(=S)−OH	−511.445375	−0.1402	0.2206	28.2873
HC(=O)−SH	−511.449325	−0.1391	0.2608	27.7830
HC(=S)−SH	−834.086649	−0.1532	0.1996	43.4183

[a] All values are in au.

fragments and to investigate whether this approach can be used to discuss reordering of the electronic density due to the bonding process.

To relate the molecular chemical potential to those of the constituent atoms, Sanderson proposed the electronegativity equalization principle, which states that all the constituent atoms (or fragments) in a molecule have the same electronegativity value given by the geometric mean of the electronegativity of the pertinent isolated atoms (or fragments).[47] In terms of the chemical potential we have

$$\mu^\circ = -\left(\prod_x^{n_f} |\mu_x^\circ|\right)^{1/n_f} \tag{6}$$

where n_f is the number of nonbonded fragments used to form the whole molecule and μ_x° is the chemical potential of fragment *x*. In this paper $n_f = 2$ and the nonbonded fragments are the monomeric units that form the hydrogen-bonded complex, so μ° is expected to give an approximation to the chemical potential of the complex that is in turn determined using the supermolecule approach. We define the associated hardness differentiating μ° with respect to the total number of electrons *N*:

$$\eta^\circ = \left(\frac{d\mu^\circ}{dN}\right)_{v(r)} = \frac{\mu^\circ}{n_f}\sum_x^{n_f}\frac{\eta_x^\circ}{\mu_x^\circ} \tag{7}$$

with η_x° being the hardness of fragment *x*. This is in fact an extension of the Sanderson's principle to hardness.[48] The difference between these approximate values with respect to the actual values should be attributed to relaxation of the electron density after bonding, quantification of this difference may help understand the reordering of the electron density as the reaction takes place.

Characterization of Transition States of 2PT Reactions. We will rationalize a 2PT process as a chemical reaction of the type $\mathbf{R} \rightarrow (\mathbf{TS})^\ddagger \rightarrow \mathbf{P}$ where reactants (**R**) transition states (**TS**) and products (**P**) are connected by an intrinsic internal reaction coordinate (IRC), through this defining the profiles of energy, chemical potential, hardness, and polarizability[39,45] that allows one to characterize the properties of the transition state. To rationalize the energy of the TS we use the Marcus equation that was originally proposed to characterize electron-transfer processes and later on used for interpretation of different kinds of chemical reactions.[36−39,50] Thus the energy barrier $\Delta E^\ddagger$ for a 2PT process is assumed to be given by

$$\Delta E^\ddagger = \frac{1}{4}K + \frac{1}{2}\Delta E^\circ + \frac{(\Delta E^\circ)^2}{4K} \tag{8}$$

with *K* being a parameter that is an intrinsic property of the reaction, $\Delta E^\circ \equiv [E(P) - E(R)]$ is the energy difference between reactants and products; $\Delta E^\ddagger \equiv [E(TS) - E(R)]$ is the barrier height measured from the reactants. From the knowledge of ΔE°
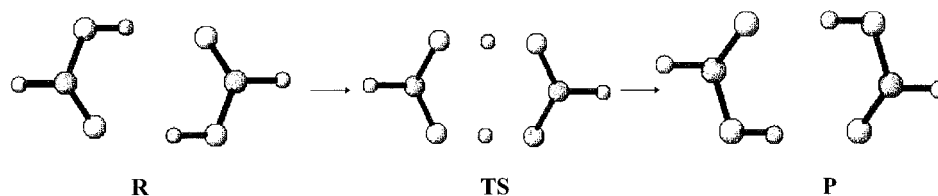
Figure 1. Schematic reaction diagram for double-proton transfer.

TABLE 2: Reference Energy (E) of the 10 Fully Optimized Bimolecular Complexes; Formation Energy (ΔE_{hb}), Chemical Potential, and Hardness from the RHF Calculation (μ,η) and from Sanderson's Rule ($\mu°, \eta°$)^a

complex	E	ΔE_{hb}	μ	$\mu°$	η	$\eta°$
HC(=O)−OH···HC(=O)−OH (**1**)	−377.664112	−0.0231	−0.1503	−0.1554	0.3204	0.3138
HC(=O)−OH···HC(=O)−SH (**2**)	−700.284742	−0.0149	−0.1402	−0.1470	0.2609	0.2863
HC(=O)−OH···HC(=S)−OH (**3**)	−700.283997	−0.0181	−0.1411	−0.1476	0.2251	0.2652
HC(=O)−OH···HC(=S)−SH (**4**)	−1022.917548	−0.0104	−0.1601	−0.1543	0.2021	0.2563
HC(=O)−SH···HC(=O)−SH (**5**)	−1022.907575	−0.0089	−0.1331	−0.1391	0.2607	0.2608
HC(=S)−OH···HC(=S)−OH (**6**)	−1022.902674	−0.0119	−0.1462	−0.1402	0.2169	0.2206
HC(=O)−SH···HC(=S)−OH (**7**)	−1022.906790	−0.0121	−0.1320	−0.1397	0.2215	0.2408
HC(=S)−SH···HC(=O)−SH (**8**)	−1345.542487	−0.0065	−0.1511	−0.1460	0.2000	0.2319
HC(=S)−SH···HC(=S)−OH (**9**)	−1345.538872	−0.0069	−0.1604	−0.1466	0.1966	0.2108
HC(=S)−SH···HC(=S)−SH (**10**)	−1668.176971	−0.0037	−0.1576	−0.1532	0.1965	0.1996

^{a} All values are in au.

and $\Delta E^{\ddagger}$ we can obtain the parameter K that in turn we use to determine the position of the TS along the IRC. Indeed the position of the TS with respect to reactants and products is obtained through the Brønsted coefficient β that was originally defined by Leffler as[51]

$$\beta = \left(\frac{\partial \Delta E^{\ddagger}}{\partial \Delta E°}\right) \Rightarrow \beta = \frac{1}{2} + \frac{\Delta E°}{2K} \tag{9}$$

where β takes values between zero and one, being one-half in the case of isoenergetic reactions ($\Delta E° = 0$). This equation is in fact a quantitative statement of the Hammond Postulate[52] since if $\Delta E° > 0$ (endothermic reaction) then $\beta > \frac{1}{2}$ and the TS is closer to products, whereas if $\Delta E° < 0$ (exothermic reaction) then $\beta < \frac{1}{2}$ and the TS is closer to reactants. Note that to characterize the position of the TSs we do not need an explicit definition of the reaction coordinate, β being a relative index representing the degree of resemblance of the transition state with respect to the products.

Recently we have proposed the following expression for the energy barrier in terms of the electronic properties μ and η[39]

$$\Delta E^{\ddagger} = \frac{1}{2}Q_{\eta}\Delta\mu^{\ddagger} + \frac{1}{2}Q_{\mu}\Delta\eta^{\ddagger} \tag{10}$$

where $\Delta\mu^{\ddagger} \equiv [\mu(TS) - \mu(R)]$ and $\Delta\eta^{\ddagger} \equiv [\eta(TS) - \eta(R)]$ and Q_{η}, Q_{μ} are parameters that have been related to the amount of electronic charge transferred during the chemical reaction. These parameters can be determined numerically as[39]

$$Q_{\eta} = \frac{(\Delta E^{\ddagger} - \Delta E°)}{(\Delta\mu^{\ddagger} - \Delta\mu°)} \tag{11}$$

and

$$Q_{\mu} = \frac{(\Delta E^{\ddagger} - \Delta E°)}{(\Delta\eta^{\ddagger} - \Delta\eta°)} \tag{12}$$

The validity of the principle of maximum hardness leads to opposite curvature for the energy and hardness; this leads to a negative Q_{μ}.[38,39] It is important to mention that eq 10 is valid when $\Delta E° = 0$ although it remains to a good approximation valid for $\Delta E° \neq 0$ provided that the parameters Q_{η} and Q_{μ} be

well defined. Equation 10 is in fact a particular case of

$$E(\omega) = \frac{1}{2}Q_{\eta}\mu(\omega) + \frac{1}{2}Q_{\mu}\eta(\omega) \tag{13}$$

that for a reaction coordinate ω is an unique expression accounting for the μ and η dependence of E for isoenergetic reactions. In cases where it is not possible to define independently the parameters Q_{μ} and Q_{η}, we will use the approximation $Q_{\mu} = -Q_{\eta}^2$ that results as a consequence of the PMH and from the dimensional analysis of eq 10 in consistency with the Parr and Pearson's expression for the energy of an atom in a molecule with constant external potential.[30]

3. Results and Discussion

Computational Details. All calculations were performed at the restricted Hartree−Fock (RHF) level of theory with the standard 6-311G** basis set using the Gaussian 94 package.[53] The profiles of E, μ, η, and α for double proton transfer in two reference systems, namely, formic acid and dithioformic acid dimers, were obtained through single points calculations of the fully optimized structures indicated by the IRC procedure. The electronic chemical potential and molecular hardness have been calculated by applying eqs 3 and 4, respectively.

Formation Reactions. Among the various bimolecular structures that are possible, we will review here only cyclic complexes where double proton transfer is possible as indicated in Figure 1. Pair combinations of monomeric units of formic (HCO−OH), dithioformic (HCS−SH), thiol−formic (HCO−SH), and thione−formic (HCS−OH) acids, leads to four dimers among the ten cyclic bimolecular complexes that will be studied here. In Table 1 we display reference values of energy, chemical potential, and hardness together with the polarizability of the different monomeric units. Formation of the complex from two isolated units involves a change in the total energy of the system together with the reordering of the electronic density favoring the stabilizing hydrogen bonds interactions. The effect of the bonding potential is apparent when comparing the change in energy, chemical potential and hardness. Table 2 displays the total energy for the hydrogen-bonded complexes together with their formation energy and electronic properties μ and η obtained from the ab initio calculations and from Sanderson's rule (eqs 6 and 7).
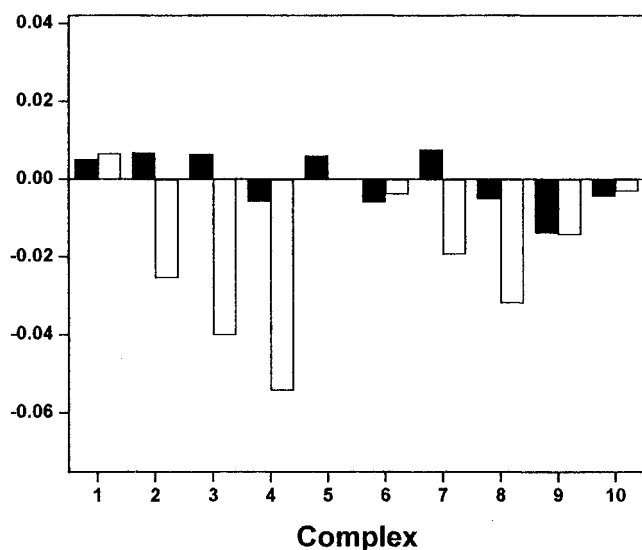
Figure 2. Deviation of the Sanderson's chemical potential (black bars) and hardness (white bars) with respect to the calculated ab initio supermolecule values of 10 bimolecular complexes labeled as in Table 2. All values are in au.
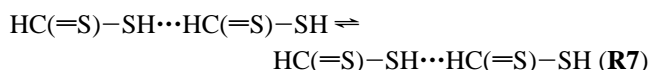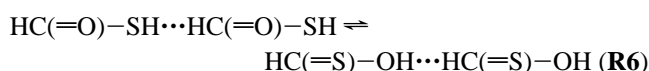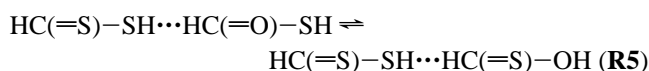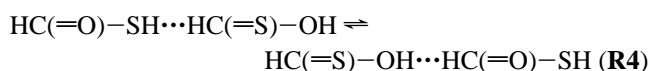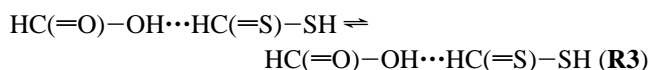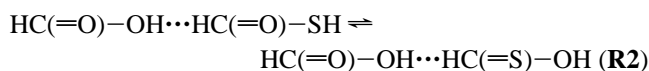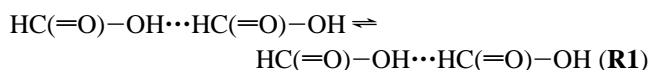
We first note that all ΔE_{hb} values fall within the energy interval defined by the dimerization energy of the reference dimers **1** and **10**. In all cases formation of the bimolecular complex is a favorable process leading to complex species in which the strength of the hydrogen bonds can be qualitatively determined from the dimerization energies, the larger is the absolute value of ΔE_{hb} the stronger are the hydrogen bonds stabilizing the complex. It appears that the bond strengths are ordered as O−H···O > O−H···S > S−H···O > S−H···S. This observation will be discussed later in connection with the barriers for proton transfer. On the other hand, the values of μ° and η° are reasonably close to the corresponding calculated values with quite small deviations $\Delta\mu = (\mu - \mu^\circ)$ and $\Delta\eta = (\eta - \eta^\circ)$ as it is apparent in Figure 2. It is interesting to mention here that numerical values of hardness calculated from eq 7 compares satisfactorily with values determined from others treatments.[54,55] For instance, we have estimated the hardness from the arithmetic average principle for softness [$S^\circ = (\sum_x S_x^\circ)/n_f$; $\eta^\circ = 1/S^\circ$][54] and the geometric mean principle for the hardness [$\eta^\circ = (\prod_x \eta_x^\circ)^{1/n_f}$][55] obtaining results that are very close to our η° displayed in Table 2, the maximum deviation detected was about 5%. Our results concerning this point indicate that there is no a dramatic reordering of the electronic density on complexation and that Sandersons rule is adequate for predicting both μ and η of the composite system. Unfortunately we have found no evidence of direct correlation between ΔE_{hb}, which contains the relaxation energy when the dimer species is formed, and $\Delta\mu$ and $\Delta\eta$, which must include at least some extent of the effect of redistribution of the electronic density.

2PT Reactions. From the monomeric units it is possible to generate ten bimolecular hydrogen bonded structures, among them there are seven nonredundant double proton-transfer reactions:

HC(=O)−OH···HC(=O)−OH ⇌

HC(=O)−OH···HC(=O)−OH (**R1**)

HC(=O)−OH···HC(=O)−SH ⇌

HC(=O)−OH···HC(=S)−OH (**R2**)

HC(=O)−OH···HC(=S)−SH ⇌

HC(=O)−OH···HC(=S)−SH (**R3**)

HC(=O)−SH···HC(=S)−OH ⇌

HC(=S)−OH···HC(=O)−SH (**R4**)

HC(=S)−SH···HC(=O)−SH ⇌

HC(=S)−SH···HC(=S)−OH (**R5**)

HC(=O)−SH···HC(=O)−SH ⇌

HC(=S)−OH···HC(=S)−OH (**R6**)

HC(=S)−SH···HC(=S)−SH ⇌

HC(=S)−SH···HC(=S)−SH (**R7**)

In Table 3 we display various TS properties of the seven 2PT reactions. We first note that most reactions are isoenergetic and thus $\Delta E^\circ = 0$. There are only three endoenergetic reactions **R2**, **R5**, and **R6** as indicated in the table. The barrier for proton transfer appear to be ordered increasingly from reaction **R1** to reaction **R7**; it is interesting to note that $\Delta E^\ddagger$ exhibits a nice proportionality with the total number of electrons of the bimolecular complex (N), as shown in Figure 3a. Note that since there are three complexes with $N = 64$ in Figure 3a we display the corresponding average value of $\Delta E^\ddagger$.

Using the optimized values of $\Delta E^\ddagger$ and ΔE° in eq 8 we have determined the K parameters that are quoted in Table 3 with the result that they are ordered as the energy barriers. Now we use eq 9 to determine the Brønsted coefficient that, as already mentioned, indicates the position of the TS along the reaction coordinate relative to reactants and products. The results of $\beta = 0.50$ or $\beta > 0.50$ show that the TS are either at midway between **R** and **P** if the reaction is isoenergetic or closer to the products if the reaction is of the endoenergetic type; this is in agreement with the Hammond postulate[52] and validates the use of eq 8 in the characterization of transition states.

Also quoted in Table 3 are values of chemical potential, hardness and polarizability. Note that all values are defined with respect to the reactants. For endoenergetic reactions we find that $\Delta\mu^\circ < 0$ indicating that electronic charge flows in the direction **R → P**, opposite of the direction of the proton transfer. On the other hand, relatively high values of $\Delta\mu^\ddagger$ show that the chemical potential is far from being constant, this fact is
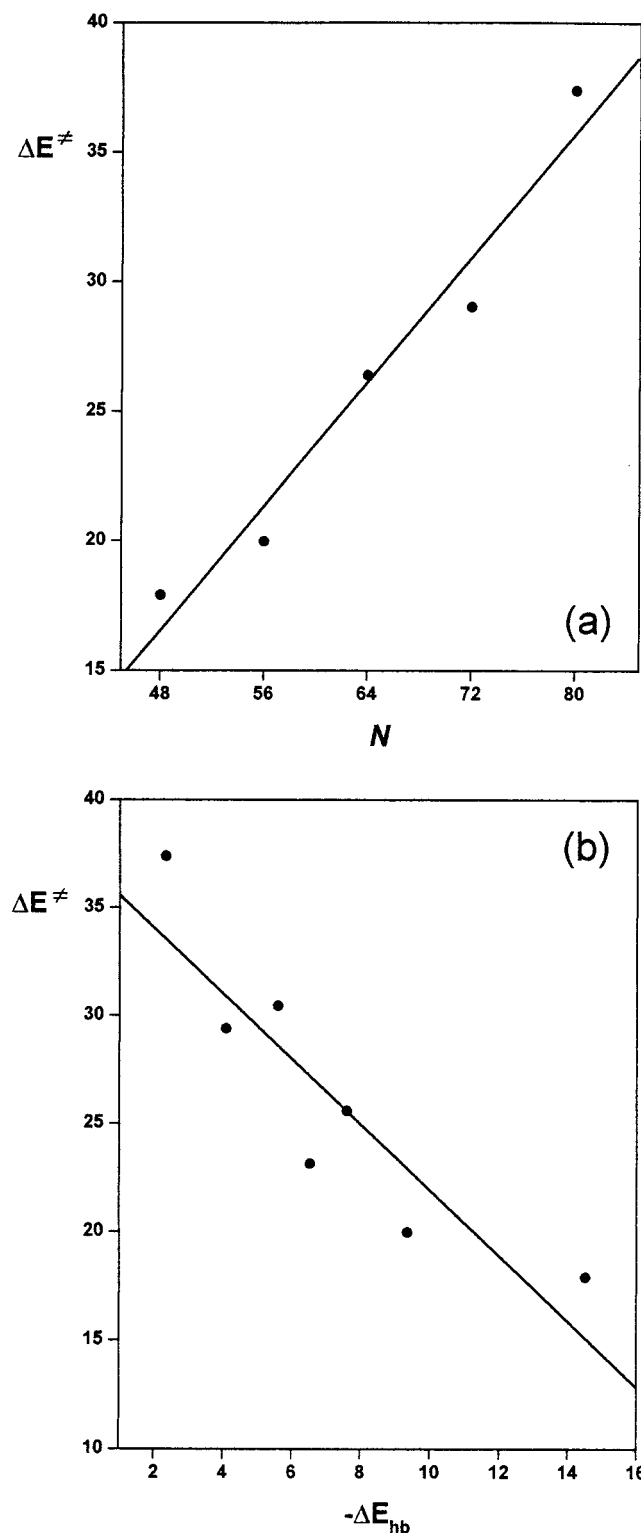
TABLE 3: Reaction Properties for Double Proton Transfer[a]

reactions	ΔE°	$\Delta E^\ddagger$	K	β	$\Delta\mu^\circ$	$\Delta\mu^\ddagger$	$\Delta\eta^\circ$	$\Delta\eta^\ddagger$	$\Delta\alpha^\circ$	$\Delta\alpha^\ddagger$	Q_η	Q_μ
R1	0.0	17.9311	71.7244	0.500	0.0	−1.7633	0.0	−6.1245	0.0	1.0890	−10.1690	−2.9278
R2	0.4675	19.9937	79.0370	0.503	−0.5397	13.3471	−22.4460	−16.5851	2.0937	4.0350	−2.0064	−4.0257
R3	0.0	23.1733	92.6932	0.500	0.0	15.4995	0.0	−4.1165	0.0	6.6230	1.4951	−5.6294
R4	0.0	25.6087	102.4348	0.500	0.0	0.8848	0.0	−4.0725	0.0	9.1603	28.9429	−6.2882
R5	2.2685	29.0499	111.6165	0.510	−5.8672	5.9613	−2.1586	−14.3700	2.1844	11.9334	−2.2288	−4.9677
R6	3.0754	30.4612	115.6122	0.513	−8.2329	−9.2056	−27.5288	−15.2422	4.2687	6.6884	−1.7199	−2.9582
R7	0.0	37.3895	149.5580	0.500	0.0	−1.9327	0.0	−7.7497	0.0	17.6313	−19.3457	−4.8246

[a] E, μ, and η are in kcal/mol; α is in au.

Double-Proton Transfer

J. Phys. Chem. A, Vol. 104, No. 5, 2000 **999**

Figure 3. Correlation between the barrier to proton transfer (in kcal/mol) with: (a) the total number of electrons of the complex and (b) the formation energy (in kcal/mol).

Figure 4. Energy, chemical potential, hardness and polarizability profiles along the IRC for the double-proton transfer of (a) formic acid dimer and (b) dithioformic acid dimer. E, μ, and η are in kcal/mol. The right axis bears the polarizability values in au.

important when discussing the principle of maximum hardness. In all cases with $\Delta E° > 0$ we see that $\Delta\eta° < 0$ showing that reactants are harder than the products, the hardest species corresponds to the most stable one, as expected from the PMH. Also $\Delta\eta^{\ddagger} < 0$ is indicating that the TS is the softest species along the reaction coordinate. These results show that a maximum in energy corresponds to a minimum value of hardness, confirming the validity of the PMH in double-proton transfer reactions. This is new evidence that the PMH holds
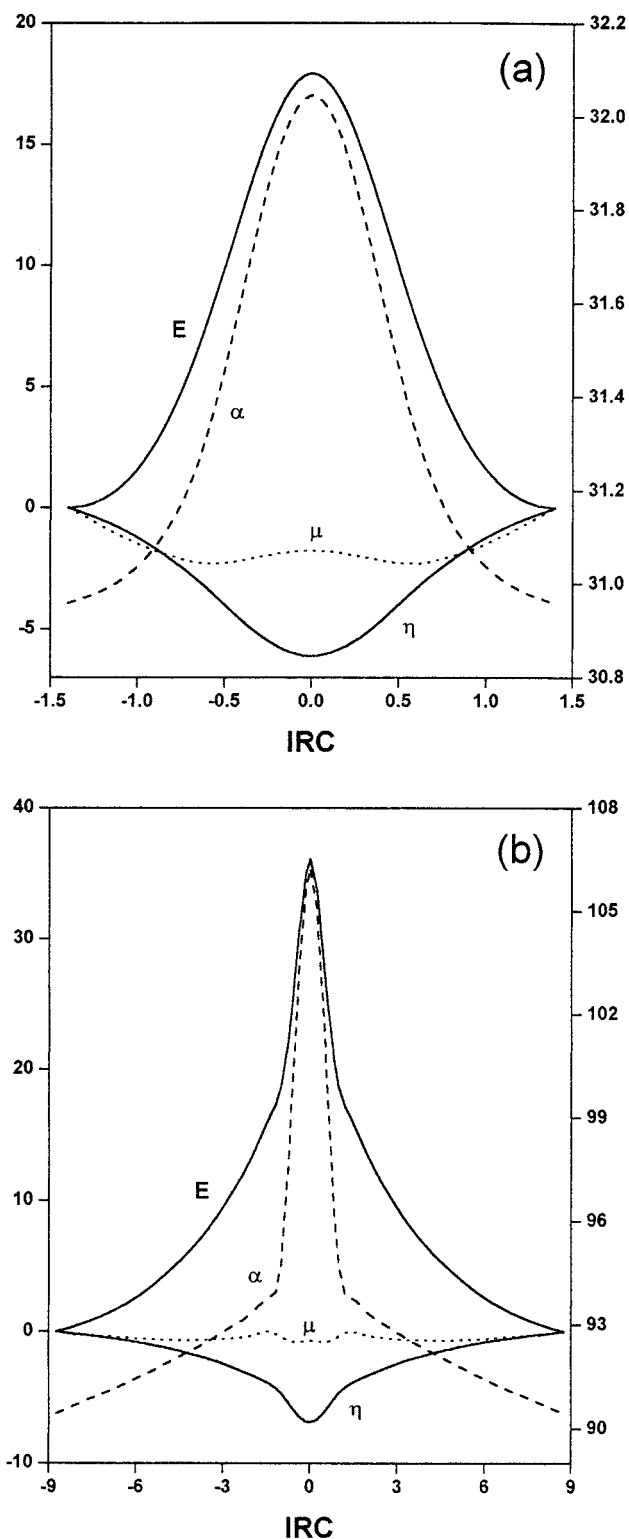
even though the chemical potential is not constant along the IRC, a condition originally imposed to prove this principle.[32,40-42]

Within the frame of DFT, a complete characterization of an N-particle wave function needs only N and the external potential $v(\bar{r})$. The response of the system to any external perturbation is measured by μ and η when N is varied for a fixed $v(\bar{r})$ as indicated by eqs 1 and 2. Complementary to this, the polarizability may be used in understanding the behavior of the system
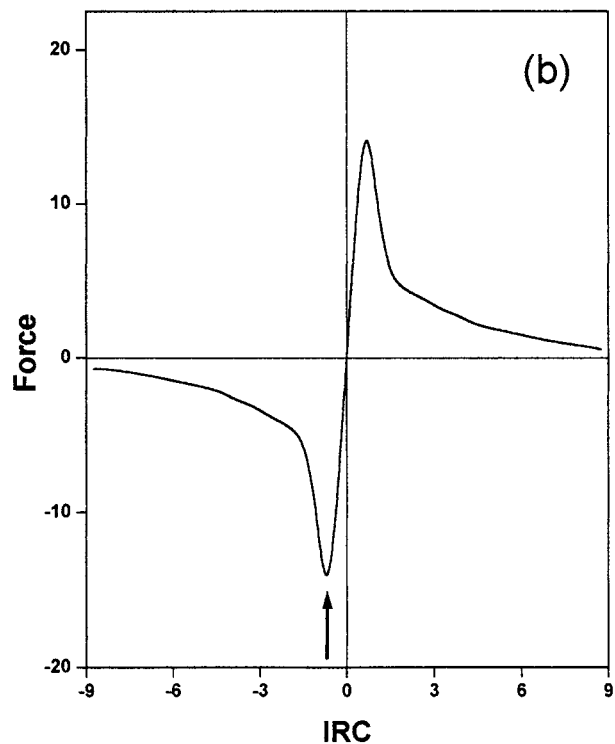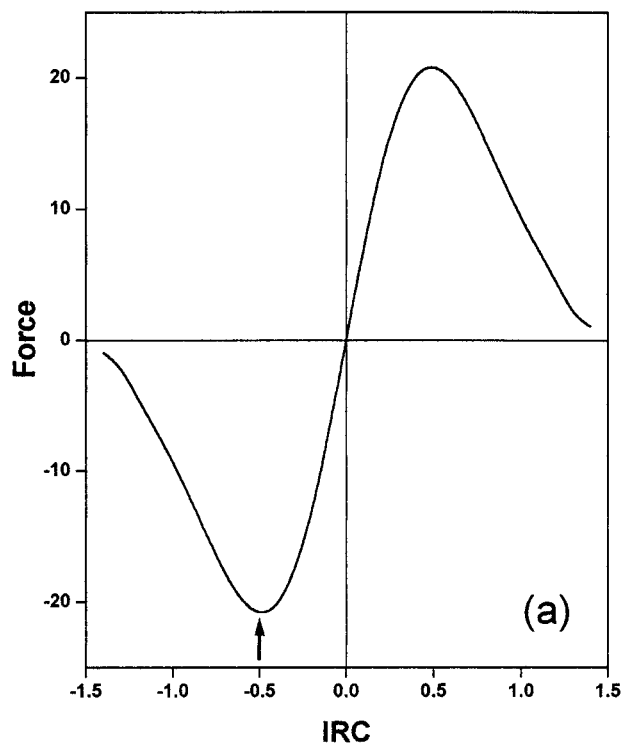
Figure 5. Profiles of the force along the IRC for (a) formic acid dimer and (b) dithioformic acid dimer. The arrows indicate the position ω_0 (see the text for details).

for changing $v(\vec{r})$ at constant N. Our results for α show that in all cases the transition state is more polarizable than the reactants showing that the minimum polarizability principle (MPP) is also satisfied in these reactions. Furthermore in all three endoenergetic reactions $\Delta\alpha° > 0$ confirming that the direction of evolution of these systems is toward the state of minimum energy and polarizability, as required by the MPP.[45]

We have defined the transition state in terms of its energy, chemical potential, and hardness, all related by eq 10 through
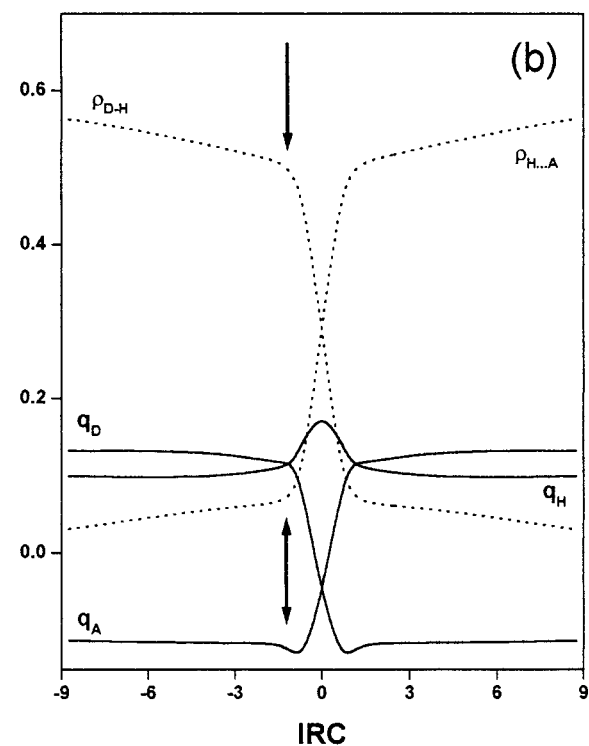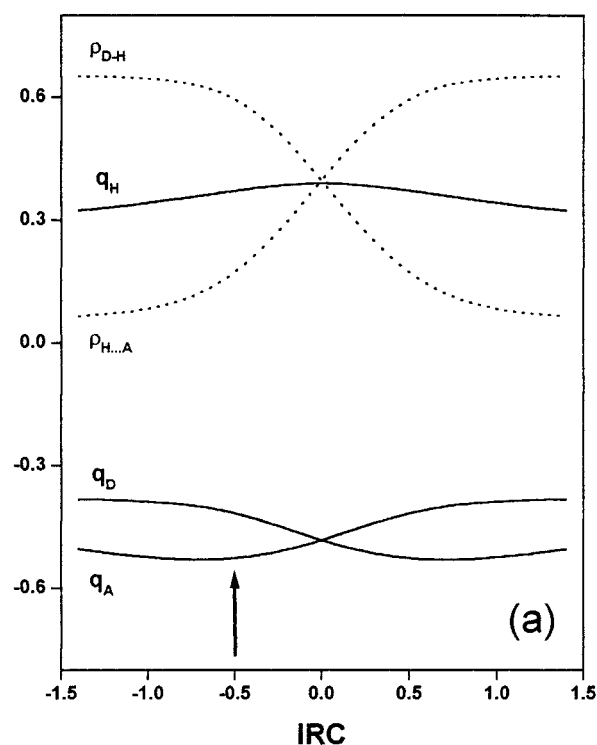

Figure 6. Profiles along the IRC of specific electronic populations of (a) formic acid dimer and (b) dithioformic acid dimer. ρ_{D-H} and $\rho_{H\cdots A}$ states the population associated with the hydrogen donor (D) and acceptor (A) regions. The arrows indicate the position ω_0 (see the text).

the parameters Q_η and Q_μ that are determined from eqs 11 and 12 and displayed in Table 3. For the endoenergetic reactions (reactions **R2**, **R5**, and **R6**) the use of eqs 11 and 12 leads to results that violate the condition that Q_μ should be negative to comply with the PMH. So in these three reactions we have assumed that $Q_\mu = -Q_\eta^2$ as suggested from the exact definitions of μ and η and the dimensional analysis of eq 10 in consistency with the Parr and Pearson expression for the energy

Double-Proton Transfer

J. Phys. Chem. A, Vol. 104, No. 5, 2000 **1001**

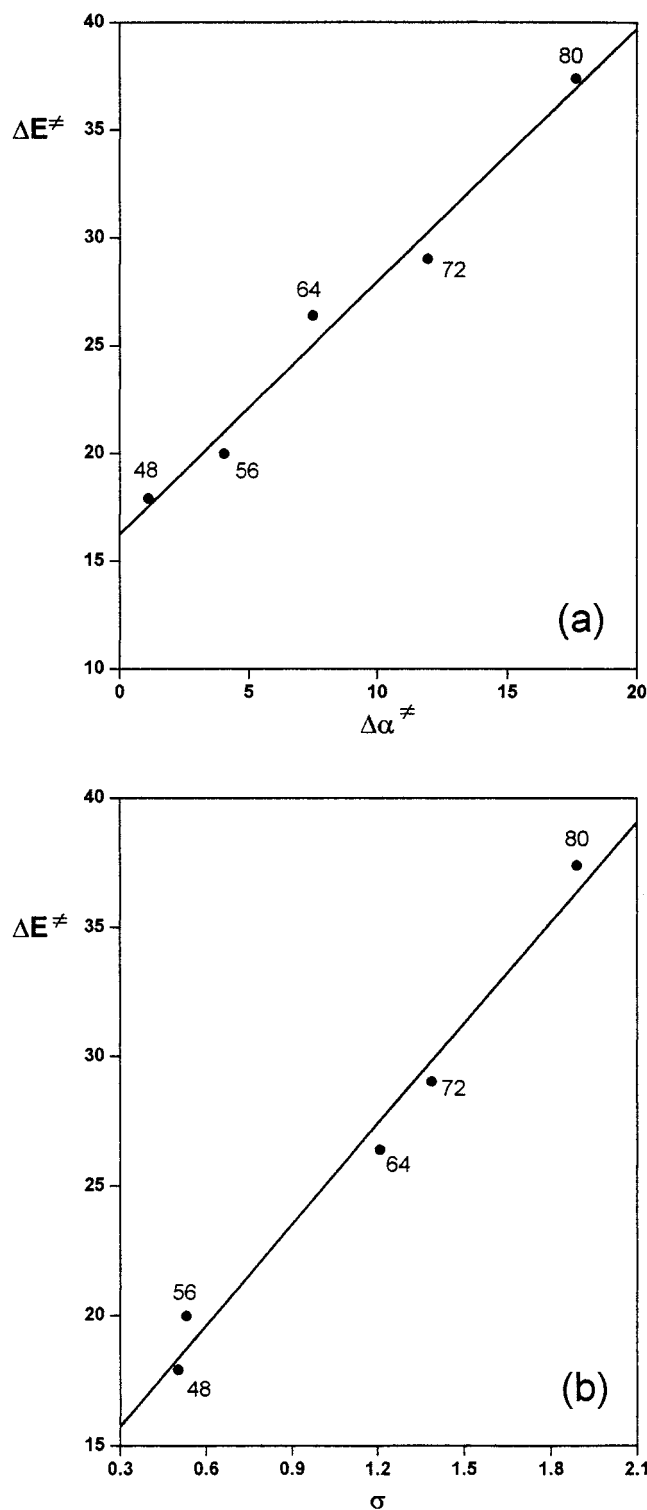**Figure 7.** Correlation between the 2PT barrier (in kcal/mol) with: (a) the activation polarizability (in au) and (b) the HSAB parameter σ for the different complexes identified by their total number of electrons.

of an atom in a molecule.[30] The resulting set of parameters that connect the properties of transition states are also included in Table 3. It is important to mention that eq 10 has been used to rationalize the activation energy of different kind of processes;[38,56] for example, for internal rotation and inversion reactions we have reported values of Q_μ going from -0.90 to -0.30.[38,56] In electrophilic aromatic substitutions processes, Zhou and Parr [57] have found proportionality between $\Delta E^\ddagger$ and $\Delta \eta^\ddagger$; their proportionality parameter was equal to -2, a value within the order of Q_μ's quoted in Table 3.

Relation Between Formation and 2PT Processes. We are dealing here with two different processes that take place sequentially; formation of the hydrogen-bonded cyclic complex followed by double-proton transfer. Although these processes seems to be independent to each other, we have found a fairly good linear correlation between the values of $\Delta E^\ddagger$ and ΔE_{hb}, as shown in Figure 3b. Large barriers to proton transfer are associated with a small complexation energy, so the stronger is the hydrogen bond, the lower is the barrier to proton transfer indicating that enhanced binding may occur when the protons gets dynamically delocalized. On the other hand, it is interesting to mention that the constant factor of the approximate linear equation relating $\Delta E^\ddagger$ and ΔE_{hb} is 37.072 kcal/mol which is very close to the 2PT barrier of the dithioformic acid dimer (37.390 kcal/mol). This result suggests that within an acceptable error marge all barriers of this series of bimolecular complexes can be written in terms of this reference value.

2PT Reaction Mechanism. In the case of the dimers formed by formic and dithioformic acids we have performed single-point calculations along the reaction coordinate to obtain the profiles of energy, chemical potential, hardness, and polarizability displayed in Figure 4. We first note in both reactions μ presents intermediate values between E and η. As can be seen, the profiles of μ decreases to reach a quite flat region around the TS, where three critical points can be perceived. The peculiar behavior of μ might be confirming the mechanism proposed in which the proton transfer is initiated by the displacement of the whole monomeric structures to favor the subsequent proton transfer. The profiles of η and α indicate the simultaneous validity of the principles of maximum hardness and minimum polarizability. We see that the hardness profiles present opposite behavior with respect to the energy whereas the polarizability profiles show maximum values at the TS's. Transition state structures are therefore characterized through a maximum value of energy and polarizability and a minimum value of hardness, as required by the PMH and MPP.

The concept of reaction mechanism is related to the notion of molecular structure in that any reactive process can be represented by nuclear displacements of the molecular system in going from the reactants to the products. These displacements are related with the forces acting on the system to bring reactants into products: this force depends only on the position along the reaction coordinate and from eq 13; it is given by[39]

$$F(\omega) = -\frac{dE}{d\omega} = -\frac{1}{2}Q_\eta\frac{d\mu}{d\omega} - \frac{1}{2}Q_\mu\frac{d\eta}{d\omega} \qquad (14)$$

expression that will be used only for qualitative purposes. In Figure 5 we display the force profiles determined by numeric differentiation of the energy profiles given in Figure 4. Note that $F(\omega)$ is negative in the reactants region and it is positive in the products region, allowing us to distinguish the different processes taking place along the reaction coordinate. Within the reactants region an activation process is taking place to attain the TS whereas in the product region we have a relaxation process from the TS. Now we use eq 14 for a qualitative rationalization of this observation: it indicates that activation processes are driven by the chemical potential term [$F(\omega) < 0 \Rightarrow Q_\eta d\mu/d\omega > |Q_\mu|d\eta/d\omega$], whereas the relaxation process is driven by the hardness term [$F(\omega) > 0 \Rightarrow Q_\eta d\mu/d\omega < |Q_\mu|d\eta/d\omega$].[39]

The profiles of the force present a minimum and a maximum around the TS, and this may be defining a region where the specific interactions and intermolecular reordering is of different nature than those encountered at the vicinity of reactants and
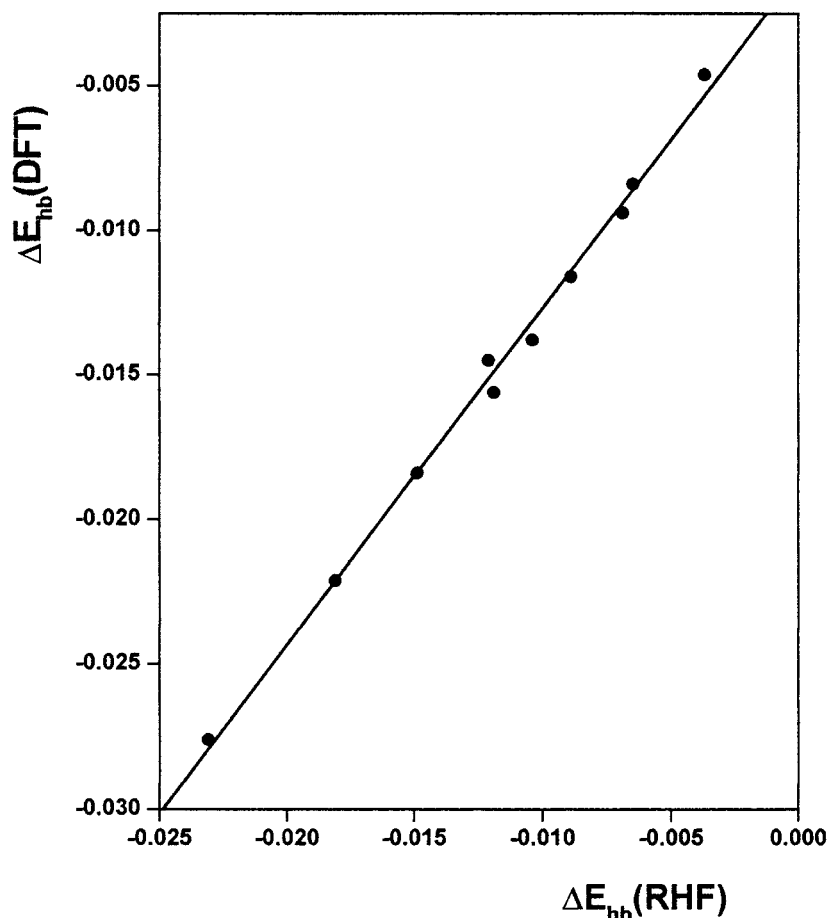
Figure 8. Comparison of DFT and RHF formation energy for the series of 10 bimolecular hydrogen-bonded complexes. All values are in au.

products, as already suggested from the peculiar profiles of the chemical potential (μ has at least three critical point at the vicinity of the TS). The results for F and μ suggest that the first step of the reaction requires an amount of work (W_1) necessary to bring the monomeric units closer to each other that is larger that the work (W_2) required for the hydrogenic motion. The associated works are qualitatively defined as $W_1 = \int_{-\infty}^{\omega_0} F(\omega) d\omega$ and $W_2 = \int_{\omega_0}^{0} F(\omega) d\omega$, with ω_0 the position of the minimum of $F(\omega)$, as indicated by the arrows in Figure 5 where it is apparent that $W_1 > W_2$ indicating that the overall reaction is determined by the first step, i.e., the motion of monomeric units to get closer to each other in order to allow the proton transfer.

Nature of 2PT Potential Barriers. To get more insight on the reaction mechanisms and the nature of potential barriers, a quantitative characterization of the electronic population in bond regions and atomic (or fragments) centers along the reaction coordinate is necessary. The Mulliken population in relevant bond regions and atomic centers along the IRC are displayed in Figure 6. The evolution of the electronic populations in bond (ρ_{X-H}) and hydrogen bond ($\rho_{X\cdots H}$) topological regions follow opposite trends; when a proton is transferred, ρ_{X-H} decreases whereas $\rho_{X\cdots H}$ increases, indicating that there is a charge transfer in the opposite direction to the proton motion. It is interesting to note that the most noticeable changes in these populations occurs after the point ω_0 (indicated by the arrows on the figures), in the region where the process is mainly proton transfer. On the other hand, in formic acid dimer the proton charge increases slightly even at the TS as shown in Figure 6a, whereas in the dithioformic dimer this quantity is quite constant but from ω_0 it suddenly increases to attain a maximum at the TS (Figure

6b). The atomic population in proton donor ($X-$) and proton acceptor ($=X$) atoms in formic acid dimer are quite close to each other favoring delocalization of the protons among the oxygens. In the case of $(HCSSH)_2$ the situation is opposite, here the difference of electronic population of donor and acceptor atoms is much more marked indicating that electrostatic and polarization interactions may be playing an important role in stabilizing the complex.

The above results suggest that the barrier for proton transfer in the formic acid dimer is roughly of *through bond* nature whereas that of dithioformic acid dimer is basically due electrostatic interactions, a *through space* barrier. Qualitatively, *through bond* interactions occur among partners that present similar local electronic population whereas *through space* interactions occurs among partners presenting quite different local electronic populations, and this is the reason this later interaction is commonly associated to non-bonded interactions. Recently we have shown that the analysis of the electronic populations and dipole moments helps characterize the nature of potential barriers.[56] In the present case however this is not possible because formic acid and dithioformic acid dimers have inversion centers and therefore their dipole moments are equal to zero all along the IRC. In the absence of permanent dipole moments we can use the polarizability to perform the qualitative analysis we require. The polarizability of a molecule is proportional to its size or to its number of electrons; Table 3 indicates that this proportionality also holds for the difference $\Delta\alpha^{\ddagger}$ (but not for $\Delta\alpha^{\circ}$). On the other hand, Figure 3a indicates that $\Delta E^{\ddagger}$ is proportional to N, so we expect it to be also proportional to $\Delta\alpha^{\ddagger}$. Figure 7a shows a good linear correlation between $\Delta E^{\ddagger}$ and $\Delta\alpha^{\ddagger}$ for the complexes identified by their total

Double-Proton Transfer

J. Phys. Chem. A, Vol. 104, No. 5, 2000 **1003**

number of electrons (for $N = 64$ we have used the average values of the properties of reactions R3, R4, and R6). We see that high barriers are associated to high values of $\Delta\alpha^{\ddagger}$ indicating that they are mostly of *through space* nature whereas low barriers are associated to low $\Delta\alpha^{\ddagger}$ values indicating that their nature is mostly of the *through bond* type.

Through bond interactions can be explained by means of the local version of the well-known Pearson's hard−soft acid−base (HSAB) principle.[58] The local HSAB principle, invoked to explain soft−soft interactions,[59−61] states that the interaction between two species occurs through atoms having nearly equal softness. The local HSAB principle provide an independent criterium in terms of specific interactions proton acceptor to characterize the nature of potential barriers. Gazquez and Mendez[59] have defined a quantity which provides the information we need:

$$\sigma = (S_{H1}^{\circ} - S_{A1}^{\circ})^2 + (S_{H2}^{\circ} - S_{A2}^{\circ})^2 \qquad (15)$$

where S_X° is the local softness of the atom X [hydrogen (H) or the corresponding acceptor (A)] defined from the global softness as $S_X^{\circ} = \rho_X \, S/N$. If the specific interactions can be explained in terms of the local HSAB principle, then σ should be small because the softness of the interacting partners are expected to be close to each other (the *soft likes soft* part of the HSAB). So large values of σ indicate that the interaction is more of the *through space* type. In Figure 7b we display a nice correlation between the 2PT barrier and the σ parameter. The result shows that the barrier for formic acid dimer can be explained in terms of the HSAB principle (small σ) confirming its *through bond* nature. Dithioformic acid dimer is the opposite, it present a relatively large value of σ confirming that its 2PT barrier is mainly of *through space* nature. It should be possible to classify the physical origin of the barriers for proton transfer of the five remaining systems as weighted averages of these two extrema.

DFT Calculations. Finally, with the purpose to validate our results we have performed DFT/B3LYP[62] calculations using the RHF optimized molecular structures to determine formation energies. The results reproduce the same trends of the Hartree−Fock calculations as illustrated in Figure 8 that shows a beautiful linear correspondence between the DFT and RHF results.

References and Notes

(1) Melander, L.; Saunders, W. H. J. *Reaction Rates of Isotopic Molecules*; John Wiley & Sons: New York, 1980.

(2) Jeffrey, G. A.; Saenger, W. *Hydrogen-Bonding in Biological Structures*; Springer-Verlag: Berlin, 1991.

(3) Scheiner, S. *Hydrogen Bonding: A Theoretical Perspective*; Oxford University Press: New York, 1997.

(4) Scheiner, S. *J. Mol. Struct. (Theochem)* **1994**, *307*, 65.

(5) Pérez, P.; Contreras, R.; Vela, A.; Tapia, O. *Chem. Phys. Lett.* **1997**, *269*, 419.

(6) Pudzianowski, A. T. *J. Chem. Phys.* **1996**, *100*, 4781.

(7) Platts, J. A.; Laidig, E. *J. Phys. Chem.* **1996**, *100*, 13455.

(8) Latajka, Z.; Bouteiller, Y.; Scheiner, S. *Chem. Phys. Lett.* **1995**, *234*, 159.

(9) Wei, D.; Salahub, D. R. *J. Chem. Phys.* **1994**, *101*, 7633.

(10) Sim, F.; St-Amant, A.; Papai, I.; Salahub, D. R. *J. Am. Chem. Soc.* **1992**, *114*, 4391.

(11) Kumar, G. A.; Pan, Y.; Smallwood, C. J.; McAllister, M. A. *J. Comput. Chem.* **1998**, *19*, 1345.

(12) Loerting, T.; Lied, K. H. *J. Am. Chem. Soc.* **1998**, *120*, 12595.

(13) Bertie, J. E.; Michaelian, K. H.; Eysel, H. H.; Hager, D. *J. Chem. Phys.* **1986**, *85*, 4779.

(14) Bertie, J. E.; Michaelian, K. H. *J. Chem. Phys.* **1982**, *76*, 886.

(15) Wilson, C. C.; Shankland, N.; Florence, A. J. *J. Chem. Soc., Faraday Trans.* **1996**, *92*, 5051.

(16) Turi, L. *J. Phys. Chem.* **1996**, *100*, 11285.

(17) Qian, W.; Krimm, S. *J. Phys. Chem.* **1996**, *100*, 14602.

(18) Qian, W.; Krimm, S. *J. Phys. Chem. A* **1998**, *102*, 659.

(19) Miura, S.; Tuckerman, M. E.; Klein, M. L. *J. Chem. Phys.* **1998**, *109*, 5290.

(20) Meyer, R.; Ernst, R. R. *J. Chem. Phys.* **1987**, *86*, 784.

(21) Shida, N.; Barbara, P. F.; Almlof, J. *J. Chem. Phys.* **1991**, *94*, 3633.

(22) Kim, Y. *J. Am. Chem. Soc.* **1996**, *118*, 1522.

(23) Lim, J.-H.; Lee E. K.; Kim, Y. *J. Phys. Chem. A* **1997**, *101*, 2233.

(24) Chajnacki, H. *Mol. Eng.* **1997**, *7*, 161.

(25) Rabold, A.; Bauer, R.; Zundel, G. *J. Phys. Chem.* **1995**, *99*, 1889.

(26) Toro-Labbé, A.; Cárdenas, C. *Int. J. Quantum Chem.* **1987**, *32*, 685. Toro-Labbé, A. *J. Mol. Struct. (Theochem)* **1988**, *180*, 209.

(27) Smeyers, Y. G.; Villa, M.; Cárdenas-Jirón, G. I.; Toro-labbé, A. *J. Mol. Struct. (Theochem)* **1998**, *426*, 155.

(28) Delaere, D.; Raspoet, G.; Nguyen, M. T. *J. Phys. Chem. A* **1999**, *103*, 171.

(29) Parr, R. G.; Yang, W. *Annu. Rev. Phys. Chem.* **1995**, *46*, 701.

(30) Parr, R. G.; Pearson, R. G. *J. Am. Chem. Soc.* **1983**, *105*, 7512.

(31) Pearson, R. G. *J. Am. Chem. Soc.* **1985**, *107*, 6801.

(32) Pearson, R. G. *J. Chem. Educ.* **1987**, *64*, 561.

(33) Parr, R. G.; Yang, W. *Density Functional Theory of Atoms and Molecules*, Oxford University Press: New York, 1989.

(34) Dreizlrer, R. M.; Gross, E. K. V. *Density Functional Theory*; Springer: Berlin, 1990.

(35) Chattaraj, P. K.; Nath, S.; Sannigrahi, A. B. *J. Phys. Chem.* **1994**, *98*, 9143.

(36) Cárdenas-Jirón, G. I.; Lahsen, J.; Toro-Labbé, A. *J. Phys. Chem.* **1995**, *99*, 5325.

(37) Cárdenas-Jirón, G. I.; Toro-Labbé, A. *J. Phys. Chem.* **1995**, *99*, 12730.

(38) Cárdenas-Jirón, G. I.; Gutiérrez-Oliva, S.; Melin, J.; Toro-Labbé, A. *J. Phys. Chem. A* **1997**, *101*, 4621.

(39) Toro-Labbé, A. *J. Phys. Chem. A* **1999**, *103*, 4398.

(40) Parr, R. G.; Chattaraj, P. K. *J. Am. Chem. Soc.* **1991**, *113*, 1854. Chattaraj, P. K.; Liu, G. H.; Parr, R. G. *Chem. Phys. Lett.* **1995**, *237*, 171. Chattaraj, P. K. *Proc. Indian Natl. Sci. Acad.* **1996**, *62*, 513.

(41) Pearson, R. G. *Chemical Hardness*; Wiley-VCH: Oxford, 1997.

(42) Datta, D. *J. Phys. Chem.* **1992**, *96*, 2409.

(43) Pross, A. *Theoretical & Physical Principles of Organic Reactivity*; John-Wiley & Sons: New York, 1995.

(44) Chattaraj, P. K.; Sengupta, S. *J. Phys. Chem.* **1996**, *100*, 16126. Chattaraj, P. K.; Poddar, A. *J. Phys. Chem. A* **1998**, *102*, 9944. Chattaraj, P. K.; Poddar, A. *J. Phys. Chem. A* **1999**, *103*, 1274.

(45) Chattaraj, P. K.; Fuentealba, P.; Jaque, P.; Toro-Labbé, A. *J. Phys. Chem. A.* **1999**, *103*, 9307.

(46) Baum, J. O.; Finney, J. L. *Mol. Phys.* **1985**, *55*, 1097.

(47) Sanderson, R. T. *Science* **1955**, *121*, 207. Sanderson, R. T. *Chemical Bonds and Bond Energy*, 2nd ed.; Academic Press: New York, 1976.

(48) Cárdenas-Jirón, G. I.; Toro-Labbé, A. *J. Mol. Struct. (Theochem)* **1997**, *390*, 79.

(49) Marcus, R. A. *Annu. Rev. Phys. Chem.* **1964**, *15*, 155.

(50) Dodd, J. A.; Brauman, J. I. *J. Phys. Chem.* **1996**, *90*, 3559.

(51) Leffler, J. E. *Science* **1953**, *117*, 340.

(52) Hammond, G. S. *J. Am. Chem. Soc.* **1955**, *77*, 334.

(53) Frisch, M. J.; Trucks, G. W.; Schlegel, H. B.; Gill, P. M. W.; Johnson, B. G.; Robb, M. A.; Cheeseman, J. R.; Keith, T. A.; Peterson, G. A.; Montgomery, J. A.; Raghavachari, K.; Al-Laham, M. A.; Zakrzewski, V. G.; Ortiz, J. V.; Foresman, J. B.; Ciolowski, J.; Stefanov, B. B.; Nanayakkara, A.; Challacombe, M.; Peng, C. Y.; Ayala, P. Y.; Chen, W.; Wong, M. W.; Andres, J. L.; Reploge, E. S.; Gomperts, R.; Martin, R. L.; Fox, D. J.; Binkley, J. S.; Defrees, D. J.; Baker, J.; Stewart, J. P.; Head-Gordon, M.; González, C.; Pople, J. A. *Gaussian 94*; Gaussian, Inc.: Pittsburgh, PA, 1995.

(54) Yang, W.; Lee, C.; Ghosh, S. K. *J. Phys. Chem.* **1985**, *89*, 5412.

(55) Chattaraj, P. K.; Nandi, P. K.; Sannigrahi, A. B. *Proc.−Indian Acad. Sci., Chem. Sci.* **1991**, *103*, 583.

(56) Gutiérrez-Oliva, S.; Letelier, J. R.; Toro-Labbé, A. *Mol. Phys.* **1999**, *96*, 61.

(57) Zhou, Z.; Parr, R. G. *J. Am. Chem. Soc.* **1990**, *112*, 5720.

(58) Pearson, R. G.; Songstad, J. *J. Am. Chem. Soc.* **1967**, *89*, 1827. Pearson, R. G. *Inorg. Chem.* **1984**, *23*, 4675; *J. Chem. Educ.* **1987**, *64*, 1987.

(59) Gázquez, J. L.; Méndez, F. *J. Phys. Chem.* **1994**, *98*, 459.

(60) Damoun, S.; Van de Woude, G., Méndez, F.; Geerlings, P. *J. Phys. Chem. A* **1997**, *101*, 886.

(61) Sengupta, D.; Chandra, A. K.; Nguyen, M. T. *J. Org. Chem.* **1997**, *62*, 6404.

(62) Becke, A. D., *J. Chem. Phys.*, **1992**, 98, 1372. Lee, C.; Yang, W.; Parr, R. G. *Phys. Rev. B*, **1988**, *37*, 785.